RSC Advances

ROYAL SOCIETY OF CHEMISTRY

www.rsc.org/advances

Thermal and electroactive shape memory behaviors of poly(L-lactide)/thermoplastic polyurethane blend induced by carbon nanotubes

Li-na Shao, Jian Dai, Zhi-xing Zhang, Jing-hui Yang, Nan Zhang, Ting Huang, Yong Wang*

School of Materials Science & Engineering, Key Laboratory of Advanced Technologies of Materials (Ministry of Education), Southwest Jiaotong University, Chengdu, 610031, China

Abstract: Poly(L-lactide) (PLLA) based shape memory materials (SMP) recently attract much attention due to their great potential application in biomedical materials. In this work, we introduced carbon nanotubes (CNTs) into a blend of PLLA/thermoplastic polyurethane (TPU) through a simple melt compounding processing to develop a new kind of PLLA SMP. The effects of CNTs on morphologies of blend composites, the selective location of CNTs, the dynamic mechanical properties of samples and the microstructure of CNTs in the blend composites were characterized using a scanning electron microscope (SEM), a transmission electron microscope (TEM) and rheological measurements, respectively. The results demonstrated that CNTs selectively located in the TPU component and induced apparent change of the blend composite morphology. High content of CNTs also formed the percolated network structure in the material, which resulted in the dramatic decrease of electrical resistivity. The shape memory behaviors of the samples were comparatively investigated in two different conditions, i.e. thermally activated and electrically activated conditions. It was demonstrated that CNTs prevents the thermally activated shape recovery process of the blend composites, especially when CNTs formed the percolated network structure. However, with the aid of electrical actuation, largely accelerated shape recovery process and enhanced degree of shape recovery were achieved for the blend composites containing 5 wt% CNTs, especially at relatively low recovery temperatures. The main mechanism was attributed to the largely enhanced electrical conductivity, which provides more Joule heating in the sample. This work provides an alternative way to develop PLLA-based shape memory materials through a simple melt compounding processing.

Keywords: Poly(L-lactide)/thermoplastic polyurethane, carbon nanotubes, shape memory behavior

* Corresponding author: Tel: +86 28 87603042;
E-mail: yongwang1976@163.com

1. Introduction

Shape memory polymers (SMPs) are smart materials that attract much attention of researchers and have earned fast development in the past years due to the fact that they can rapidly change their shape from a temporary shape to the original shape or permanent shape under an appropriate stimulus such as solvent, pH value, temperature, light, electrical, and magnetic field, etc.[1-5] SMPs exhibit great potential applications in many fields ranging from biomedical materials, smart fabrics, and temperature sensors, information carriers, actuators to aerospace applications.[6-14] Therefore, many researches have been carried out to investigate the shape memory effects (SME) of newly-synthesized polymers or endow common polymers with shape memory behaviors so that the application fields of such polymers could be enlarged.[15,16]

Poly($_L$-lactide) (PLLA) has attracted much attention in recent years not only because of its good comprehensive mechanical properties and good processability but also because of its completely renewable resources ranging from corn, starch, and sucrose. Therefore, people hope that it can be a promising alternative to petroleum-based plastics, and then the wide application of PLLA can reduce the dependence on petrochemical products.[17] Furthermore, the other well known characteristics of PLLA are their biodegradability and biocompatibility, which endow PLLA with great potential applications in biomedical fields, such as drug carriers, tissue scaffolds, implant materials, and surgical suture, etc.[18]

The SME of PLLA or PLLA-based materials then have come into notice. So far, shape memory PLLA materials have been prepared mainly through two strategies. The first strategy is introducing a stable network structure, which usually determines the driving force for shape recovery in shape memory PLLA materials due to its entropic elasticity, in the main chain of PLLA through chemical synthesis, and in this condition, PLLA chains act as a switching unit, which is responsible for controlling the shape fixity and recovery.[19, 20] However, synthesis and characterization of new kinds of PLLA-based systems are usually complicated and inconvenient. The second strategy is relating to melt blending technology, which is thought to be an efficient and simple way to prepare new materials with optimized chemical and physical properties.[21-25] In the blends, PLLA component still provides the switch but the other component acts as the role of cross-linking structure. The introduced component is usually an elastomer. For example, Zhang W et al[25] melt-blended PLLA with a polyamide elastomer (PAE) and they found that besides the

enhancement of tensile ductility, the blends also exhibited the apparent SME.

Due to the intrinsic characteristics such as the high strength and modulus, large aspect ratio, and especially high electrical conductivity, carbon nanotubes (CNTs) are widely used to prepare electrically activated shape memory materials.[26-28] The SME of the composites are controlled by many factors, such as the content, dispersion state, and the surface modification of CNTs, etc.[28-31] For example, Jung YC et al[28] prepared polyurethane (PU)/CNT composites through different methods, including conventional blending, in situ and cross-linking polymerization methods. They found that the shape recovery of the composites was strongly influenced by the dispersed structure of CNTs. Mahapatra SS et al[31] prepared CNTs-filled hyperbranched PU (HPU) and they found that the composites exhibited an excellent shape recovery ability and a rapid recovery speed in both thermal triggering and electrical actuating shape memory behaviors. Moreover, in our previous work,[32] different contents of CNTs were introduced into a thermoplastic PU (TPU) and the results demonstrated that at room temperature, CNTs delayed the shape recovery behavior of the composites, especially when the percolated CNT network structure was formed. However, with the aid of electrical actuation, largely accelerated shape recovery behavior was achieved for the TPU/CNT sample containing 5 wt% CNTs.

Considering the potential advantages of CNTs in the polymer blends, it is interesting to ask what happens for the shape memory behavior of PLLA blend composites with the presence of CNTs. In our group, much work has been carried out to investigate the microstructure-performance relationships of CNTs filled PLLA blend composites.[33-35] Through controlling the selective location states and the contents of CNTs in different blend composites, including PLLA/TPU/CNT,[33] polycarbonate (PC)/PLLA/CNT,[34] and PLLA/ethylene-*co*-vinyl acetate (EVA)/CNT,[35] largely enhanced impact toughness, tensile ductility, and improved electrical conductivity at lower CNT content can be achieved. For example, in the PLLA/TPU/CNT blend composites, CNTs selectively locate in the TPU phase, and the impact strength at room temperature (23 ℃) increases from 6.3 kJ/m^2 of the binary PLLA/TPU (70/30) blend to 53.7 kJ/m^2 of the blend composite containing 2 wt% CNTs.[33]

In this work, we attempt to clarify the effect of CNTs on the shape memory behavior of PLLA/TPU blend. It is well known to all that TPU exhibits a great application as smart materials due to its high tunable microstructure, high strain recovery, easy processing, light weight and low

cost and therfore, many researches have been carried out to develop the TPU-based shape memory materials.[36-38] For the PLLA/TPU/CNT blend composites, the presence of TPU component endows the material with excellent mobility even if the environmental temperature is below the glass transition temperature of PLLA component on one hand. On the other hand, the presence of CNTs possibly endows the materials with good electrical conductivity and electrically activated shape memory behaviors. To realize the aim, different contents of CNTs (0-5 wt%) are introduced into PLLA/TPU (50/50, wt/wt) blend, and the thermally activated and electrically activated shape memory behaviors are comparatively investigated. Interestingly, it is observed that CNTs reduce the recovery ratio of the blend composites during the thermally activated shape recovery process while they increases the recovery ratio and accelerate the recovery process during the electrically activated shape recovery process. Considering the biodegradability and biocompatibility of PLLA, it is believed that the PLLA/TPU/CNT shape memory materials have great application as biomedical materials.

2. Experimental part

2.1 Materials

All the materials used in this work are commercially available. PLLA (2002D, with D-isomer content of 4.3%, weight-average molecular weight (M_w) of 2.53×10^5 Da, melt flow rate (MFR) of 5.6 g/10min (190 ℃/2.16 kg) and a density of 1.24 g/cm^3) was purchased from NatureWorks®, USA. Polyester-based TPU (WHT-1570) with the density of 1.19 g/cm^3 and a glass transition temperature (T_g) of about -40 ℃ was purchased from Wanhua Polyurethane Co., Ltd. (Yantai, China). It should be stressed that TPU was completely amorphous. CNTs (Flo TubesTM 9000) were purchased from CNano Technology Co., Ltd., China. The density of CNTs was 1.9 g/cm^3. The purity of CNTs was more than 95%, and the average diameter and length of a single CNT were ca. 11 nm and 10 μm, respectively.

2.2 Sample preparation

All the samples were prepared through melt compounding processing. Before melt compounding, pristine materials were dried at 50 ℃ for 24 h to eliminate the effect of moisture. After that, a master batch of TPU/CNT containing 10 wt% CNTs was first prepared, then the master batch was

diluted by melt compounding with PLLA and TPU to obtain the compositions. In this work, the weight ratio between PLLA and TPU was maintained at 50/50 (wt/wt) while the contents of CNTs varied from 1 to 5 wt%. The melt-compounding was conducted on a twin-screw extruder SHJ-30 (Nanjing Ruiya, China) at melt temperatures of 150-160-175-190-200-200-195 ℃ from hopper to die and a screw speed of 150 rpm. After that, the blend composites were compression-molded at a melt temperature of 180 ℃ and a pressure of 5 MPa to obtain the plates with a thickness of 1 mm. For a comparison, the binary PLLA/TPU blend was also prepared through the completely same processing procedures. The sample notation was named as C*x*, where *x* represented the content of CNTs in the blend composites.

2.3 Scanning electron microscopy (SEM)

Morphological characterization was conducted on a scanning electron microscope (SEM) Fei Inspect (FEI, the Netherlands) with an accelerating voltage of 5 kV. Before characterization, samples were cryogenically fractured in liquid nitrogen. Then, the cryo-fractured surfaces were characterized after being coated with a thin layer of gold.

2.4 Transmission electron microscopy (TEM)

The dispersion states of CNTs in the blend composites were further investigated through a transmission electron microscope (TEM) JEM-2100F (JEOL, Japan) with operating voltage of 200 kV. An ultrathin section with a thickness of about 120 nm, which was cut using a cryo-diamond knife on a microtome EM UC6/FC6 (LEICA, Germany), was used for TEM characterization. Before TEM characterization, the sample slice was stained by OsO_4 vapor.

2.5 Rheological measurement

A stress-controlled rheometer DHR-1 (TA Instrument, USA) was used to detect the processing flow ability of materials and the microstructure of CNTs in the blend composites. A sample disk with a diameter of 25 mm was cut from the previously compression-molded plate. The measurements were carried out at 180 ℃ and a frequency range of 0.01-100 Hz. In addition, it was stressed that the measurement was carried out in nitrogen atmosphere.

2.6 Dynamic mechanical analysis (DMA)

The glass transitions of samples were investigated through a dynamic mechanical analysis (DMA) measurement that was conducted on a DMA Q800 analyzer (TA Instrument, USA). A rectangular cross-sectional bar (with the length, width and thickness of 15, 5 and 1 mm, respectively) was cut

from the previously compression-molded plate. During the DMA measurement, a tensile mode was selected. The temperature was heated from -80 to 100 ℃ at a heating rate of 3 ℃/min and the frequency was set at 1 Hz.

2.7 Electrical resistivity measurement

The electrical resistivity of blend composites was measured using a universal meter DT9208 (Shenzhen Hongda, China). A rectangular cross-sectional bar was cut from the previously compression-molded plate. Before measurement, the two ends of the bar were coated with a thin layer of conductive silver paint to erase the influence of contact resistance, then the electrical resistivity was measured by a two-point technique. For the binary PLLA/TPU blend, because its electrical resistivity is very high, beyond the measurement range of the universal meter (200 Ω-200 MΩ), a Digital High Resistance Test Fixture PC68 (Shanghai Precision Instrument Manufacture, China) with a high resistance measurement range of 10^3-10^{17} Ω was then used.

2.8 Shape memory behavior measurement

The shape memory behavior of sample was examined by a bending test under two different conditions, i.e. thermally activated and electrically activated conditions. A breeches-like sample that was cut from the previously compression-molded plate was used for the shape memory behavior measurements. The photographs of the sample obtained at different states are shown in Figure 1. The specimen had a thickness of 1 mm, the maximum width of 15 mm, and the maximum length of 50 mm. The width and length for each leg were 5 and 25 mm, respectively. For the thermally activated shape memory behavior, the sample was first deformed at 75 ℃ (deformation temperature, T_d), and then the sample was quickly cooled to room temperature (20 ℃, fixity temperature, T_f) to fix the deformed shape. After that, the deformed sample was quickly heated to another temperature (recovery temperature, T_r) and the shape of sample gradually returned to the original shape. For the electrically-activated shape memory behavior, the two ends of the sample were then coated with a thin layer of conductive silver paint to erase the influence of contact resistance. The length of part that was coated by conductive silver paint was 5 mm. During the shape recovery process, a constant voltage of 50 V was applied and the shape recovery process was then recorded. To quantitatively describe the shape recovery behavior of

sample, two parameters, i.e. recovery ratio (R_r) and recovery speed (R_s,°/s), were roughly defined by following relations:

$$R_r = \frac{\theta_t - \theta_0}{180 - \theta_0} \times 100\% \quad (1)$$

$$R_s = \frac{\theta_t - \theta_0}{t} \quad (2)$$

Where θ_0 and θ_t represented the initially bended angles of the pre-deformed sample and actually bended angle of the recovered sample at recovery time t during the recovery process as shown in Fig. 1.

3. Results and discussion

3.1 Morphology of the blend composites and the dispersion of CNTs

The effect of CNTs on morphology of the PLLA/TPU blend was firstly investigated using SEM. As shown in Figure 2, the binary PLLA/TPU blend (C0, Fig. 2a) exhibits the typical co-continuous structure. PLLA is a brittle polymer with T_g of about 60 ℃ while TPU is a ductile polymer with T_g of -40 ℃ and therefore, one can easily differentiate PLLA from TPU component according to the surface morphological features because the two components exhibit the different fracture modes, although samples were prepared in liquid nitrogen. With the presence of CNTs (Fig. 2b-d), an apparent morphological change is observed. Namely, the phase domain of TPU component increases while the phase domain of PLLA component decreases with increasing CNT content. Specifically, at CNT content of 5 wt%, the continuity of PLLA component is greatly reduced on one hand. On the other hand, the domain of TPU component is greatly increased and it tends to become the matrix. In other words, a morphological change from the co-continuous morphology to the sea-island morphology is induced. CNTs inducing the similar morphological change in the immiscible polymer blends has been reported elsewhere.[39-41] There are two possibilities that contribute to the morphological changes. The first possibility might be related to the change of viscosity ratio between components and the second possibility to the volume-filling effect of CNTs because of the selective location of CNTs in the TPU component as demonstrated in the following.

Similar to other nanofillers, CNTs also exhibit selective location behavior in an immiscible polymer blends, and their selective location states are determined by thermodynamic interaction, which is relating to the interfacial affinity between CNTs and blend components, and the kinetic parameters, which are usually related to the viscosity ratio, blending sequence, blending time and shear stress, etc.[42-44] In this work, CNTs exhibit relatively stronger interfacial affinity to TPU component[33] and the blend composites were prepared using the master batch of TPU/CNT and therefore, either based on the thermodynamic consideration or based on the kinetic consideration, CNTs selectively locate in the TPU component. Figure 3 shows the SEM images of the blend composites obtained at relatively higher magnifications. It demonstrates that in all the blend composites, CNTs selectively locate in the TPU component. Furthermore, one can also see that the phase domain of TPU component increases with increasing CNT content. To further demonstrate the selective location of CNTs in the blend composites, the representative C5 sample was characterized using TEM. As shown in Figure 4, CNTs selectively locate in TPU component. In addition, CNTs contact each other and tend to form the network-like structure. This will be further demonstrated through the following rheological measurements.

3.2 Rheological behavior

It is well known that rheological measurement is an efficient way to provide information about the processing ability and the microstructure-performance relationship of the composites, especially the information about the microstructure of fillers in the polymer melt. For example, the presence of a plateau in storage modulus or loss modulus curve at low frequency range is an indicative of a percolated network structure of fillers formed in the melt.[45] Here, the percolated CNT network structure can be also demonstrated from the rheological results as shown in Figure 5, which shows the storage modulus, loss modulus and complex viscosity of different samples with and without CNTs. It can be seen that addition of a few number of the CNTs induces apparent changes of rheological properties at relatively lower frequencies. Specially, a plateau is really observed in modulus curves. This clearly demonstrates the formation of CNT network structure in the blend composites. The more the CNTs in the blend composites, the more apparent the changes of the rheological properties are.

3.3 Dynamic mechanical properties

The dynamic mechanical properties of samples were investigated using DMA. Figure 6a exhibits

the loss factor ($\tan\delta$) of pure PLLA, pure TPU, the binary PLLA/TPU blend and the representative blend composites. For the PLLA component, there are two features that need to be noticed. First, the binary blend and the ternary blend composites exhibit relatively smaller T_g compared with the pure PLLA possibly due to the effect of TPU component. Second, the blend composites exhibit very similar T_g to that of the binary blend, which indicates that the presence of CNTs does not apparently change the chain segment mobility of the PLLA component in the blend composites. This is possibly attributed to the selective location of CNTs in the TPU component rather than in the PLLA component. However, different from the strong loss factor peak of the pure TPU sample, the blend and/or blend composites exhibit relatively weaker loss factor peak. Namely, both the intensity ($\tan\delta_{\max}$) and the area of loss factor, which are direct indicators of the damping behavior of a given material and represent the energy dissipation during the measurement, are greatly reduced. This is possibly attributed to the restriction of PLLA component and/or CNT network structure that prevents the viscous flow of TPU molecular chains. To better understand the glass transition of the TPU component, the variations of storage modulus (E') of samples are shown in Fig. 6b. It can be seen that the presence of CNTs greatly increases the storage modulus of the blend composites, especially at temperature higher than T_g of the TPU component but smaller than T_g of the PLLA component. In addition, all the blend composites exhibit similar temperature ranges during the glass transition process to that of the binary blend.

3.4 Electrical resistivity

Due to their high electrical conductivity, CNTs have been widely used to improve the electrical conductivity of polymer materials. According to the 'percolation model", the prerequisite for a dramatic decrease in electrical resistivity is the formation of a conductive CNT network structure in the composites. In this work, CNTs selectively locate in the TPU component and the blend composites exhibit the co-continuous structure on one hand. On the other hand, CNTs form the percolated network structure at relatively high content. Therefore, it is expected that largely reduced electrical resistivity can be achieved with increasing CNT content. Figure 7 shows the variation of the volume electrical resistivity of samples versus the content of CNTs. For the binary PLLA/TPU blend, the volume electrical resistivity is bigger than 10^{14} Ω. Addition of 1 wt% CNTs

induces the great decrease of electrical resistivity and the value is smaller than 10^6 Ω. This indicates that a conductive pathway is already formed in the blend composite. Furthermore, increasing CNT content results in the further decrease of electrical resistivity. To better understand the variation of electrical property, the electrical conductivity of the PLLA/TPU blend composites was rationalized in terms of modified classical percolation scaling law:[46] $\sigma = \sigma_0 (p - p_c)^t$, where σ represents the conductivity of the composites, p is the filler content and p_c is the percolation threshold, σ_0 is a scaling factor and t is a percolation exponent which generally reflects the dimensionality of the system with values around 1.3 and 2 for two and three-dimensions, respectively. The inserted graph shown in Fig. 7 represents a best fit to experimental conductive data as a function of p - p_c. It can be seen that the blend composites exhibit p_c of 0.47 wt% and t of 1.77. This indicates that addition of only 0.47 wt% CNTs, a conductive CNT network structure can be formed in the PLLA/TPU blend composites.

3.5 Shape memory behavior

Thermally activated shape memory behaviors

The shape memory behaviors of the blend composites obtained at two different conditions, including thermally activated condition and electrically activated condition, were quantitatively analyzed through observing the shape recovery processes of the deformed samples. Figure 8 shows the initial states of the deformed samples obtained at a fixity temperature of 20 ℃ and the final states obtained after being recovered at different recovery temperatures (T_r =50, 60 and 75 ℃) for different time. It is well known to all that TPU is a typical SMP and the SME arises from the phase-separated structure of its hard and soft segments.[47-49] Generally, TPU has two typical transitions, i.e. the glass transition and melting/crystallization, which can be used as the swithing segments during the shape recovery process. In this work, TPU component is completely amorphous and therefore, only the glass transition is considered. Since the glass transition temperature (T_g) of soft segments in TPU is much lower than the room temperature and consequently, the deformed shape of TPU obtained at low temperatures can be completely recovered at temperature higher than the room temperature.

From Fig. 8 it can be seen that after being recovered at 50 ℃ for 600 sec, the binary PLLA/TPU sample exhibits a recovery ratio (R_r) of about 20%. Because the recovery temperature is lower than T_g of PLLA component and the mobility of PLLA is completely restricted, it is then believed that the driving force for shape recovery is of the entropic elasticity of the stable network of TPU component. Due to the restriction effect of PLLA component on the mobility of TPU molecular chains, the recovery of TPU is also restricted and consequently, a small R_r is achieved. For the blend composites, the shape memory behavior is dependent upon the CNT content. The C1 and C2 samples exhibit the similar R_r compared with the C0 sample, which indicates that adding a few amount of CNTs does not apparently affect the shape recovery processes of the blend composites. However, apparently decreased R_r (13%) is obtained for the C5 sample. This indicates that the shape recovery of the C5 sample is restricted or delayed. It has been demonstrated that CNTs selectively locate in the TPU component and high content of CNTs form the percolated network structure in the sample. Therefore, it is believed that the delayed shape recovery of the C5 sample is mainly attributed to the formation of the percolated CNT network structure in the TPU component, which reduces the mobility of TPU molecular chains.

Furthermore, one can see that increasing T_r facilitates the shape recovery of all the samples. The higher the T_r is, the larger the R_r is. Obviously, the restriction effect of PLLA component on mobility of TPU component is greatly weakened on one hand. On the other hand, the enhanced driving force originated from the physically crosslinked TPU component at elevated T_r also contributes to the increase of R_r. However, the restriction effect of CNT network structure on shape recovery of the blend composites is still present, especially at relatively higher CNT content.

To better understand the thermally activated shape recovery process of the samples, the variation of R_r with increasing recovery time (t) is illustrated in Figure 9. In addition, the recovery speed R_s (^{o}/s) is also indicated. From Fig. 9a one can see that at relatively lower T_r, the variation of R_r is inconspicuous, and all the samples exhibit the linear increase of R_r with increasing t.

Although the C5 sample exhibits the smallest R_r at all t, the differences in R_r among all the samples are still very small. Furthermore, one can see that all the samples exhibit very small R_s. At T_r of 60 ℃ (Fig. 9b), the C1 and C2 samples exhibit the similar variation trends of R_r versus t, indicating the similar shape recovery processes in these samples. This further demonstrates that addition of a few amount of CNTs does not affect the shape recovery of the blend composites apparently. As expected, the C5 sample exhibits relatively smaller R_r at same t compared with the other samples. Furthermore, from the variation of R_r versus t it can be deduced that the whole process of shape recovery of samples can be divided into three stages as shown in the graph. *Stage I*, the variation of R_r is very small and all the samples exhibit the similar shape recovery behaviors possibly due to the fact that it takes a few seconds to transfer heat or generate heat to the samples during the early stage of shape recovery process. In other words, the existence of the *Satge I* is possibly related to the heat transfer. *Stage II*, in a short time, R_r increases dramatically with increasing t. In this stage, most of the deformed shape is recovered. *Stage III*, the variation of R_r becomes inconspicuous again. R_s is calculated according to the variation of shape recovery in the *Stage II*. It can be seen that addition of CNTs reduces R_s of the blend composites. The more the CNTs in the blend composites, the smaller the R_s is. Similar variation trends of R_r versus t are also observed at T_r of 75 ℃ (Fig. 9c). In this condition, the restriction effect of CNTs on the shape recovery behaviors of the blend composites becomes more apparent.

Electrically activated shape memory behaviors

From Figure 10 it can be seen that for the binary blend, the electrically activated shape recovery behaviors at all T_r are very similar to the thermally activated shape recovery behaviors obtained at same T_r. This is easily to be understood because the binary sample is completely insulated and the applied voltage is very small and therefore, the effect of voltage on shape recovery behaviors of the binary blend can be completely ignored. Interestingly, for the blend composites, it is demonstrated that the shape recovery behaviors depends not only on the content of CNTs but also

on T_r. For example, at T_r of 50 ℃, the C5 sample exhibits R_r of 74%, which is much higher than that obtained during the thermally activated shape recovery process. In other words, the shape recovery of the C5 sample is greatly accelerated with the aid of external voltage. Different from the gradually increased R_r with increasing of T_r during the thermally activated shape recovery process, the blend composites exhibit similar R_r at T_r of 60 and 75 ℃ during the electrically activated shape recovery process on one hand. On the other hand, increasing CNT content promotes the shape recovery of blend composites. This means that the effect of recovery temperature on the shape recovery of blend composites is weakened and simultaneously, the restriction effect of CNT network structure on shape recovery also disappears.

Figure 11 exhibits the variations of R_r with increasing t obtained during the electrically activated shape recovery process. Compared with the results as shown in Fig. 8, there are several differences that need to be noticed. First, at T_r of 50 ℃ (Fig. 10a), the C5 sample exhibits the dramatic change of R_r with t. It also exhibits much higher R_s (1.26 ^{o}/s) compared with the other three samples. Second, with the increase of T_r (Fig. 10b and 10c), all the samples exhibit the similar three stages during the shape recovery process as mentioned above. Furthermore, increasing CNT content not only facilitates the increase of R_r at same t but also induces the increase of R_s. Third, the role of CNTs becomes inconspicuous at 75 ℃ possibly due to that the recovery temperature is high enough, and the shape recovery process of the sample is mainly determined by recovery temperature rather than by CNT content and/or external voltage.

To better understand the shape recovery behaviors at different conditions, i.e. thermally activated and electrically activated conditions, R_r and R_s of the representative C5 sample are compared in the Figure 12. From Fig. 12a one can see that at relatively lower T_r, the C5 sample exhibits more apparent electrically activated shape recovery than the thermally activated shape recovery, and much higher R_r is achieved during the electrically activated shape recovery process. However, with increasing T_r, the difference in R_r between electrically activated shape recovery

and thermally activated shape recovery becomes smaller. Interestingly, from Fig. 12b it can be seen that the C5 sample exhibits much higher R_s in the electrically activated condition than that obtained in the thermally activated condition at all T_r. This indicates that with the aid of external voltage, beside the enhanced degree of shape recovery, the shape recovery process of the C5 sample can be also greatly accelerated.

Generally, the electrically activated shape recovery is mainly related to the temperature change in the sample when the external voltage is applied. In this condition, the external voltage induces the occurrence of a phenomenon which is classically denoted as Joule heating. This indicates that the electrically activated shape effects are also thermally activated. For example, Mahapatra SS et al.[31] measured the variation in the surface temperature of the composites and found that for the HPU/CNT composites with fast shape recovery behavior, the surface temperature enhanced in a very short time when a certain voltage was applied. This indicates that a higher electrical conductivity is the prerequisite for achieving higher efficiency as a shape memory material.[15] In this work, even if the recovery temperature is below T_g of PLLA, the C5 sample exhibits the apparent shape recovery behavior with the aid of external voltage. This is very significant from a viewpoint of decreasing recovery temperature or achieving the SME at relatively lower temperatures. Obviously, this work demonstrates that the PLLA/TPU/CNT blend composites exhibit good shape memory effect either in the thermally activated condition or in the electrically activated condition. However, there are still some problems that need to be resolved in the future. For example, can shape changes be triggered at relativley lower voltage? Can larger recovery stresses be exerted by the introduced systems? How reliable is such a system when running a large number of actuation cycles? Further work will be carried to clarify these problems.

4. Conclusions

In summary, the PLLA/TPU/CNT blend composites with different CNT contents have been prepared. Morphological characterizations demonstrate that CNTs selectively locate in the TPU component, which induces the morphological change of the blend composites from co-continuous morphology to sea-island morphology. Rheological measurements demonstrate that at relatively high CNT content, CNTs form the percolated network structure in the blend composites. Addition

of CNTs greatly reduces the electrical resistivity of the sample and a percolation threshold of 0.47 wt% is achieved. Either in the thermally activated condition or in the electrically activated condition, the samples exhibit good shape memory effect. The higher the environmental temperature, the more apparent the shape memory effect is. The presence of CNTs prevents the shape recovery process of the samples, especially at relatively high CNT content. The electrically activated shape recovery also depends on environmental temperature and the content of CNTs. Even at relatively lower temperature, high content of CNTs not only enhances the degree of shape recovery but also accelerates the shape recovery process. This work provides an alternative but simple way to prepare the PLLA-based shape memory materials.

Acknowledgements

Authors express their sincere thanks to the National Natural Science Foundation of China (51473137) for financial support.

References

1 J. Hu, Y. Zhu, H. Huang and J. Lu, *Prog. Polym. Sci.*, 2012, **37**, 1720-1763.

2 D. Iqbal and M. H. Samiullah, *Materials*, 2013, **6**, 116-142.

3 G. J. Berg, M. K. McBride, C. Wang and C. N. Bowman, *Polymer*, 2014, **55**, 5849-5872.

4 X. Wu, W. M. Huang, Y. Zhao, Z. Ding, C. Tang and J. Zhang, *Polymers*, 2013, **5**, 1169-1202.

5 H. Meng and G. Li, *Polymer*, 2013, **54**, 2199-2221.

6 M. Bothe and T. Pretsch, *J. Mater. Chem. A*, 2013, **1**, 14491-14497.

7 A Khaldi, J. A. Elliott and S. K. Smoukov, *J. Mater. Chem. C*, 2014, **2**, 8029-8034.

8 L. Sun, W.M. Huang, C.C. Wang, Z. Ding, Y. Zhao, C. Tang and X.Y. Gao, *Liq. Cryst.*, 2014, **41**, 277-289.

9 M. Bothe and T. Pretsch, *Macromol. Chem. Phys.*, 2012, **213**, 2378-2385.

10 A.Y.N. Sofla, S.A. Meguid, K.T. Tan and W.K. Yeo, *Mater. Des.*, 2010, **31**, 1284-1292.

11 Y. Liu, H. Du, L. Liu and J. Leng, *Smart. Mater. Struct.*, 2014, **23**, art. no. 023001.

12 N. Fritzsche and T. Pretsch, *Macromolecules*, 2014, **47**, 5952-5959.

13 M. Ecker and T. Pretsch, *RSC Adv.*, 2014, **4**, 286-292.

14 M. Ecker and T. Pretsch, *RSC Adv.*, 2014, **4**, 46680-46688.

15 Y. J. Liu, H. B. Lv, X. Lan, J. S. Leng and S. Y. Du, *Compos. Sci. Technol.*, 2009, **69**, 2064-2068.

16 Q. H. Men and J. L. Hu, *Compos. Part A.*, 2009, **40**, 1661-1672.

17 L. T. Lim, R. Auras and M. Rubino, *Prog. Polym. Sci.*, 2008, **33**, 820-852.

18 R. M. Rasal, A. V. Janorkar and D. E. Hirt, *Prog. Polym. Sci.*, 2010, **35**, 338-356.

19 Y. F. Huang, P. J. Pan, G. R. Shan and Y. Z. Bao, *RSC Adv.*, 2014, **4**, 47965-47976.

20 M. H. Xie, L. Wang, J. Ge, B. L. Guo and P. X. Ma, *ACS Appl. Mater. Inter.*, 2015, **7**, 6772-6781.

21 C. Samuel, S. Barrau, J. M. Lefebvre, J. M. Raquez and P. Dubois, *Macromolecules*, 2014, **47**, 6791-6803.

22 J. J. Song, H. H. Chang and H. E. Naguib, *Eur. Polym. J.*, 2015, **67**, 186-198.

23 B. B. Yan, S. Y. Gu and Y. H. Zhang, *Eur. Polym. J.*, 2013, **49**, 366-378.

24 M. Raja, S. H. Ryu, A. M. Shanmugharaj, *Eur. Polym. J.*, 2013, **49**, 3492-3500.

25 W. Zhang, L. Chen and Y. Zhang, *Polymer*, 2009, **50**, 1311-1315.

26 J. W. Cho, J. W. Kim, Y. C. Jung and N. S. Goo, *Macromol. Rapid. Commun.*, 2005, **26**, 412-416.

27 H. Deka, N. Karak, R. D. Kalita and A. K. Buragohain, *Carbon*, 2010, **48**, 2013-2022.

28 Y. C. Jung, H. J. Yoo, Y. A. Kim, J. W. Cho and M. Endo, *Carbon*, 2010, **48**, 1598-1603.

29 S. Y. Gu, B. B. Yan, L. L. Liu and J. Ren, *Eur. Polym. J.*, 2013, **49**, 3867-3877.

30 N. G. Sahoo, Y. C. Jung, H. J. Yoo and J. W. Cho, *Compos. Sci. Technol.*, 2007, **67**, 1920-1929.

31 S. S. Mahapatra, S. K. Yadav, H. J. Yoo, M. S. Ramasamy and J. W. Cho, *Sensor. Actuat. B-Chem.*, 2014, **193**, 384-390.

32 J. Chen, Z. X. Zhang, W. B. Zhang, J. L. Li, J. H. Yang, Y. Wang, Z. W. Zhou and J. H. Zhang, *Mater. Des.*, 2015, **69**, 105-113.

33 Y. Y. Shi, W. B. Zhang, J. H. Yang, T. Huang, N. Zhang, Y. Wang, G. P. Yuan and C. L. Zhang, *RSC Adv.*, 2013, **3**, 26271-26282.

34 Y. H. Wang, X. L. Xu, J. Dai, J. H. Yang, T. Huang, N. Zhang, Y. Wang, Z. W. Zhou and J. H. Zhang, *RSC Adv.*, 2014, **4**, 59194-59203.

35 X. F. Wand, Z. X. Zhang, J. L. Li, J. H. Yang, Y. Wang and J. H. Zhang, *RSC Adv.*, 2015, **5**,

69522-69533.

36 O. Jaudouin, J. J. Robin, J. M. Lopez-Cuesta, D. Perrin, C. Imbert, *Polym. Int.*, 2012, **61**, 495-510.

37 L. Zhang, N. R. Brostowitz, K. A. Cavicchi, R. A. Weiss, *Macromol. React. Eng.*, 2014, **8**, 81-99.

38 T. Takahashi, N. Hayashi, S. Hayashv, *J. Appl. Polym. Sci.*, 1996, **60**, 1061-1069.

39 H. Zou, K. Wang, Q. Zhang and Q. Fu, *Polymer*, 2006, **47**, 7821-7826.

40 S. Bose, A. R. Bhattacharyya, A. P. Bondre, A. R. Kulkami and P. Pötschke, *J. Polym. Sci., Part B: Polym. Phys.*, 2008, **46**, 1619-1631.

41 F. M. Xiang, Y. Y. Shi, X. X. Li, T. Huang, C. Chen, Y. Peng and Y. Wang, *Eur. Polym. J.*, 2012, **48**, 350-361.

42 M. Sumita, K. Sakata, S. Asai, K. Miyasaka and H. Nakagawa, *Polym. Bull.*, 1991, **25**, 265-271.

43 A. Göldel, G. R. Kasaliwal, P. Pötschke and G. Heinrich, *Polymer*, 2012, **53**, 411-421.

44 Y. Y. Shi, J. H. Yang, T. Huang, N. Zhang, C. Chen and Y. Wang, *Compos. Part B.*, 2013, **55**, 463-469.

45 P. Pötschke, T. D. Fomes and D. R. Paul, *Polymer*, 2002, **43**, 3247-3255.

46 D. Stauffer and A. Aharony, Introduction to percolation theory. London: Taylor and Francis; 1994.

47 B. K. Kim, S. Y. Lee and M. Xu, *Polymer*, 1996, **37**, 5781-5793.

48 W. M. Huang, B. Yang, Y. Zhao and Z. Ding, *J. Mater. Chem.*, 2010, **20**, 3367-3381.

49 S. J. Chen, H. M. Yuan, Z. C. Ge, S. G. Chen, H. T. Zhuo and J. H. Liu, *J. Mater. Chem. C*, 2014, **2**, 1041-1049.

Figure captions:

Figure 1: Schematic representations showing the pre-deformed sample (a) and the recovered sample at recovery time t during the thermally (b) and electrically (c) activated shape recovery processes.

Figure 2: SEM images showing the morphology of the binary blend and the ternary blend composites. (a) C0, (b), C1, (c) C2, and (d) C5

Figure 3: SEM images showing the selective location of CNTs in the blend composites. (a) C1, (b) C2, and (c) C5

Figure 4: TEM images showing the selective location of CNTs in the representative blend composite containing 5 wt% CNTs. Images were taken at (a) low and (b) high magnifications.

Figure 5: Rheological properties of the samples. Storage modulus, (b) loss modulus, and (c) complex viscosity

Figure 6: (a) Loss factor ($\tan\delta$) and (b) storage modulus (E') of pure PLLA, pure TPU, the binary PLLA/TPU blend and the representative blend composites.

Figure 7: (a) Variation of electrical resistivity of the PLLA/TPU blend composites versus the content of CNTs.

Figure 8: Images demonstrating the initial state and the unconstrained bend recoverability of samples at different recovery temperatures (50, 60, and 75 ℃) for different recovery time (sec). The final recovery ratios of samples were labeled in the images.

Figure 9: Variations of the recovery ratios of different samples versus the recovery time obtained at different recovery temperatures. The recovery speed was also indicated in the graphs. (a) 50 ℃, (b) 60 ℃, and (c) 75 ℃

Figure 10: Images demonstrating the initial state and the unconstrained bend recoverability of samples at different recovery temperatures (50, 60, and 75 ℃) for different recovery time (sec). A constant voltage of 50 V was applied during the recovery process. The final recovery ratios of samples were labeled in the images.

Figure 11: Variations of the recovery ratios of different samples during the electrically activated shape recovery process versus the recovery time obtained at different recovery temperatures. (a) 50 ℃, (b) 60 ℃, and (c) 75 ℃

Figure 12: Comparison of the SME of the representative C5 sample obtained at different

conditions as shown in the graphs. (a) Recovery ratio and (b) recovery rate.

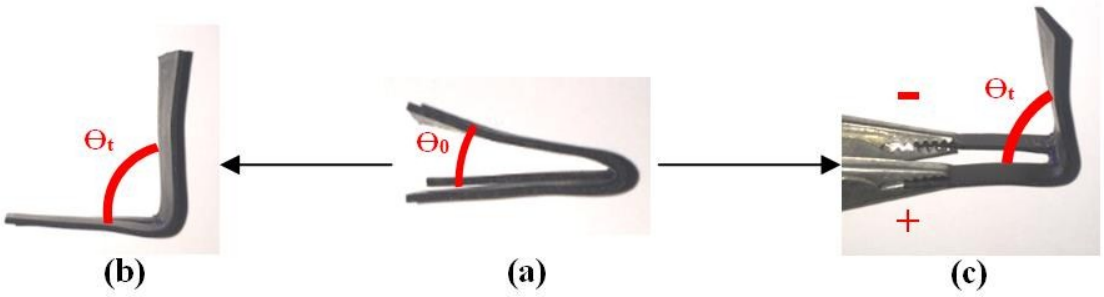

Figure 1

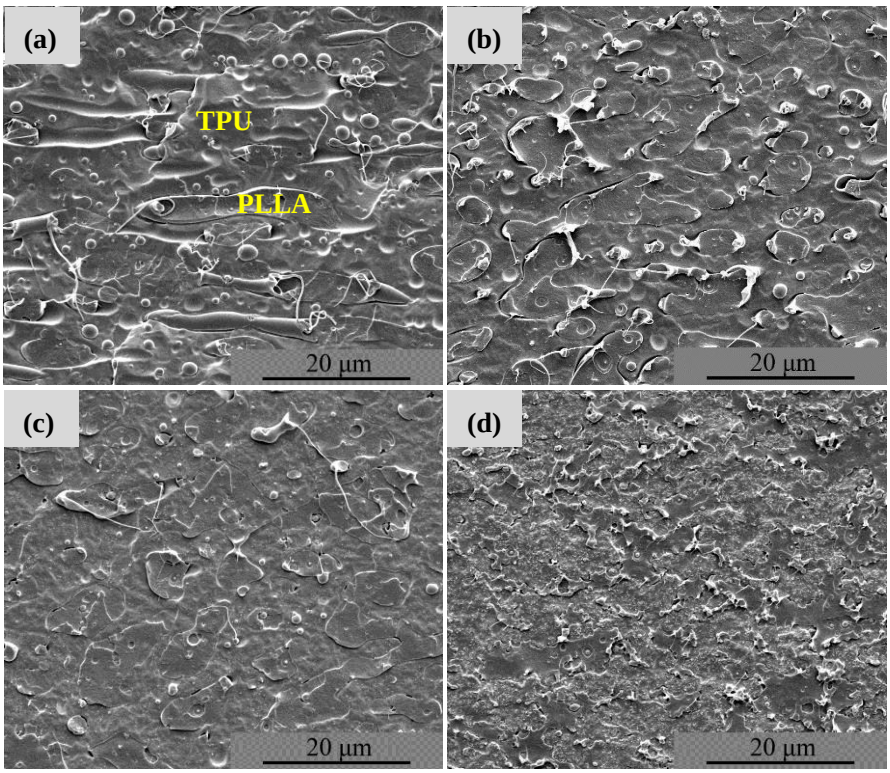

Figure 2

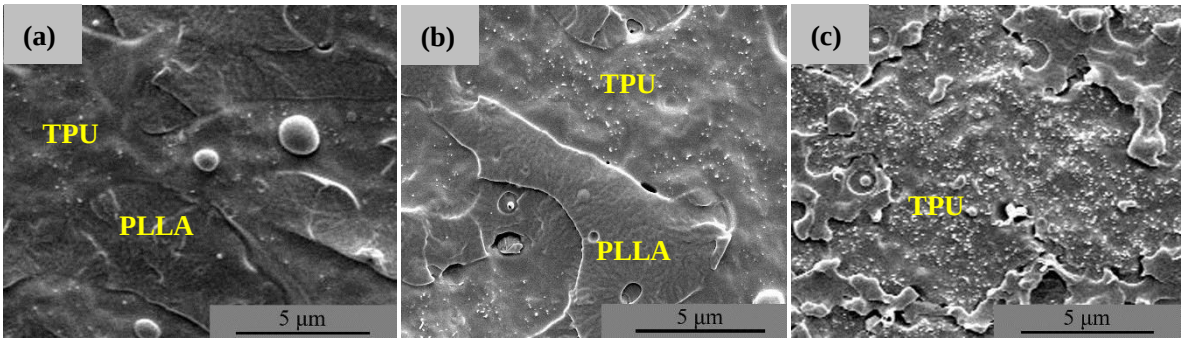

Figure 3

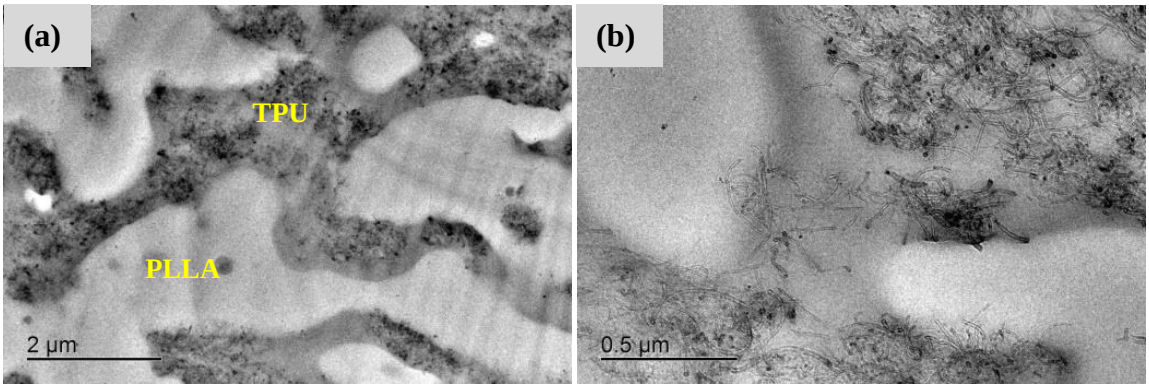

Figure 4

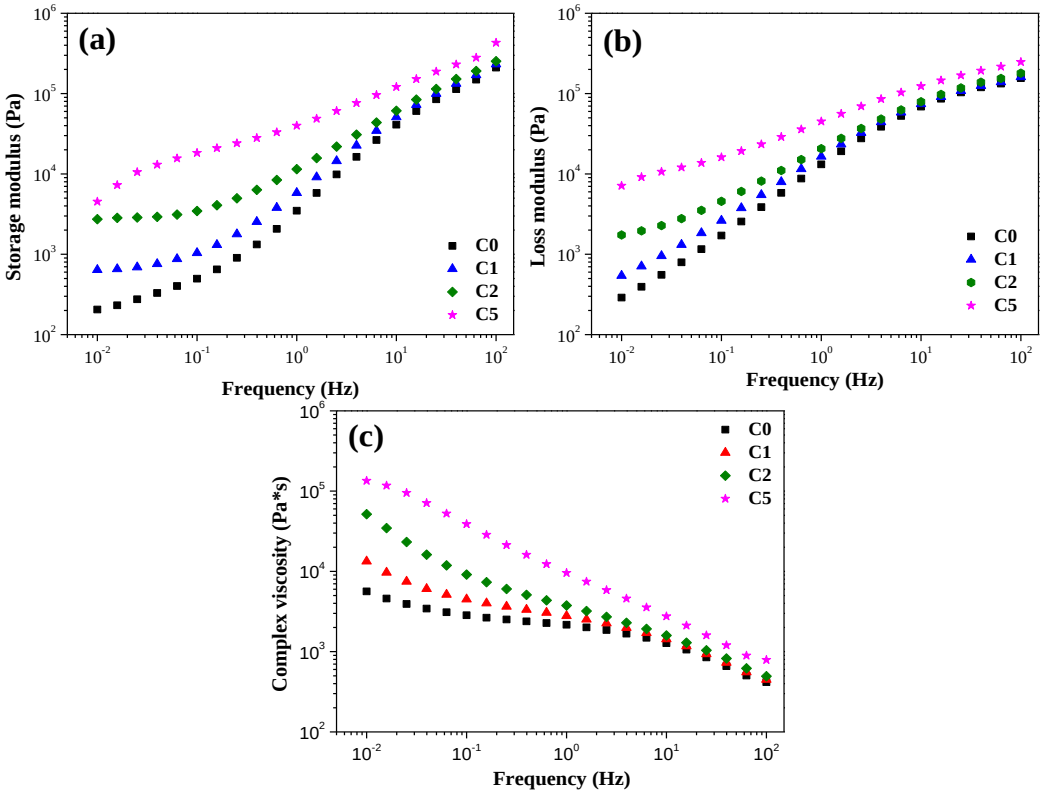

Figure 5

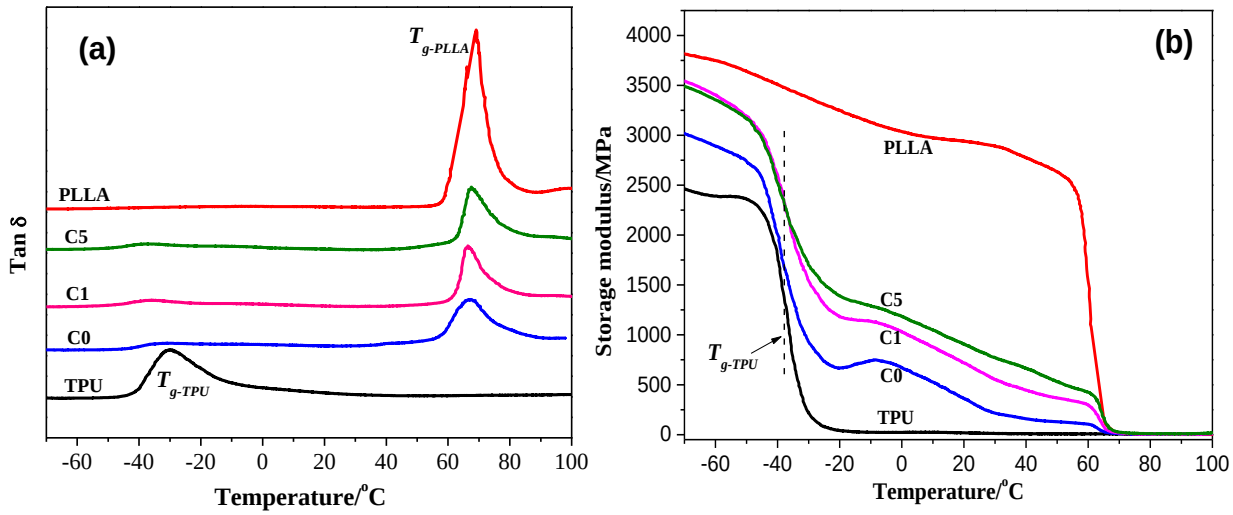

Figure 6

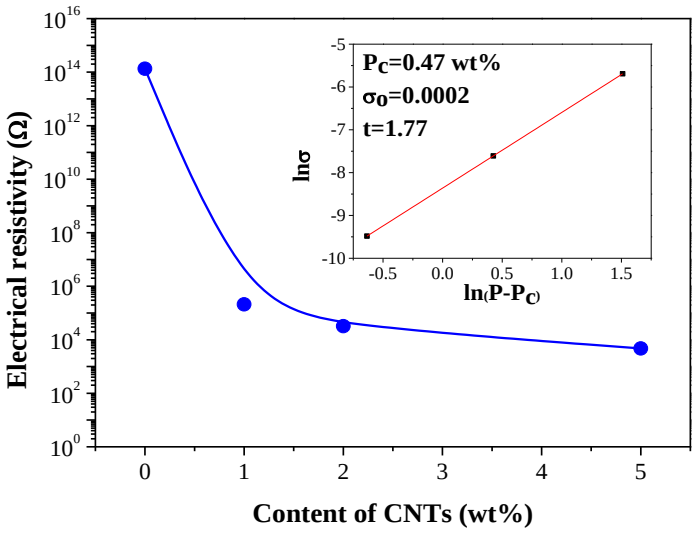

Figure 7

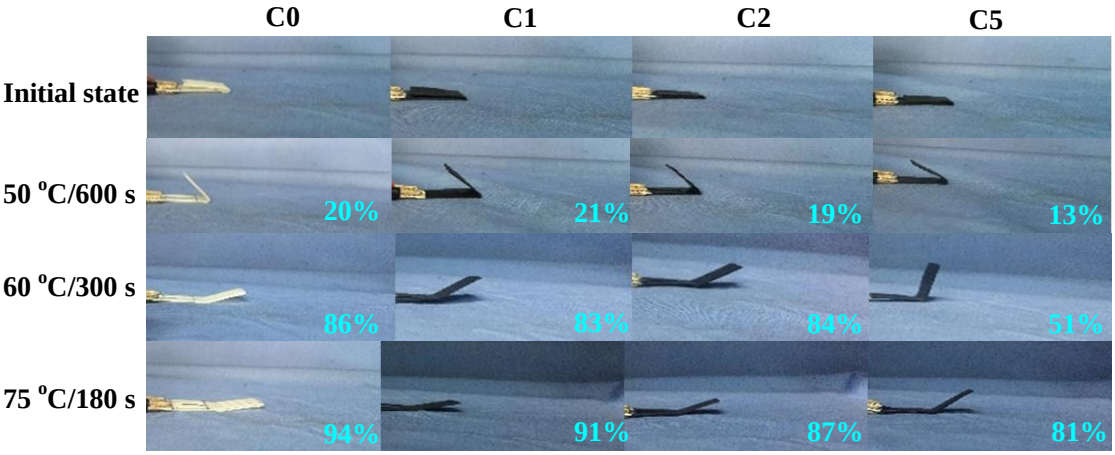

Figure 8

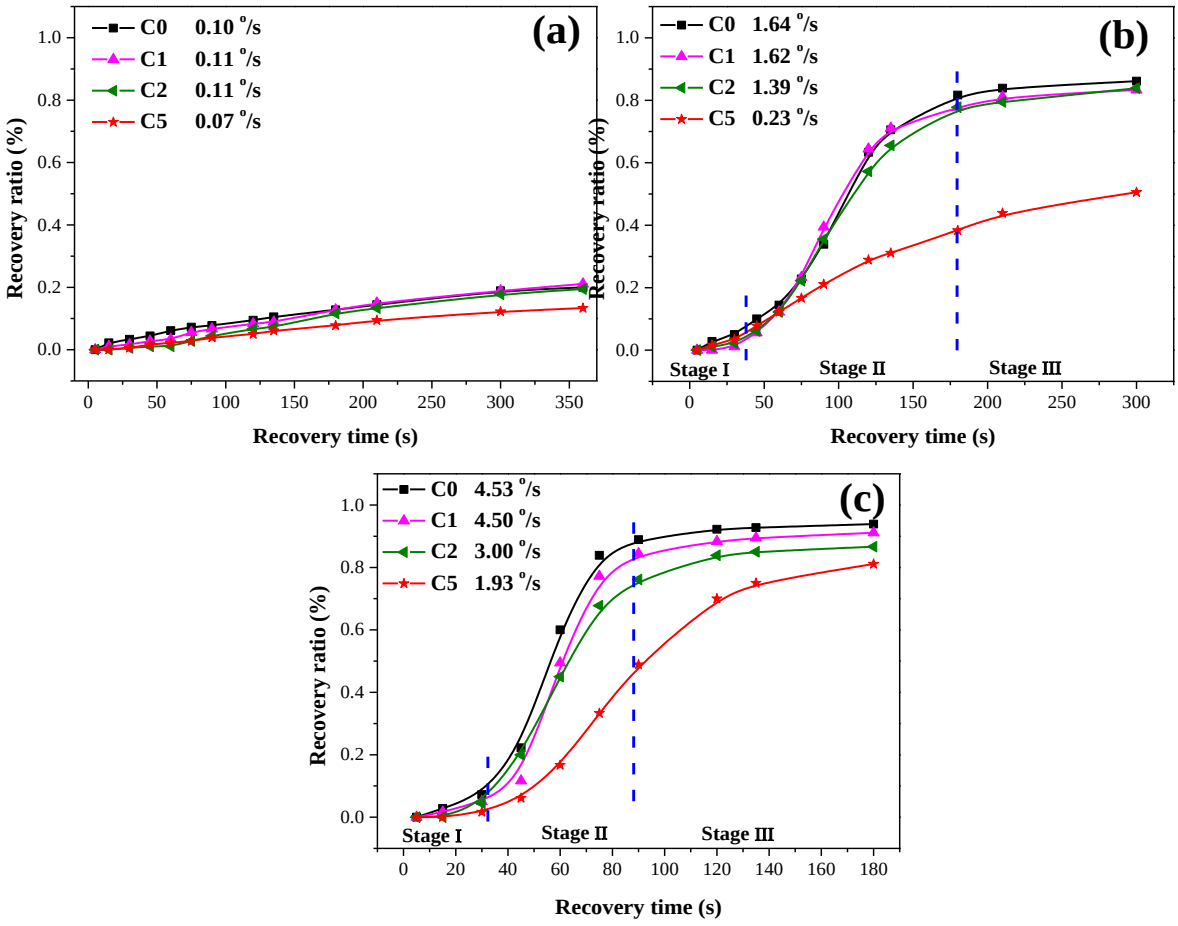

Figure 9

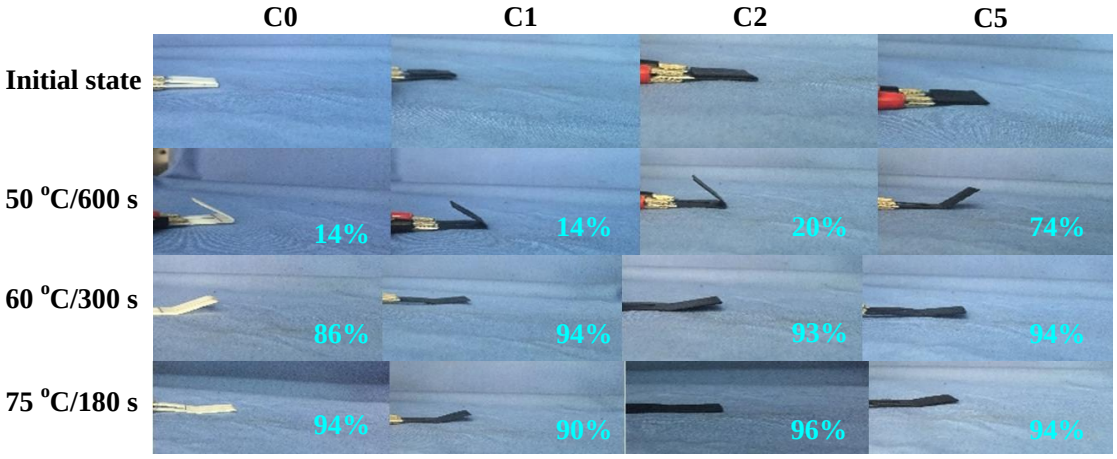

Figure 10

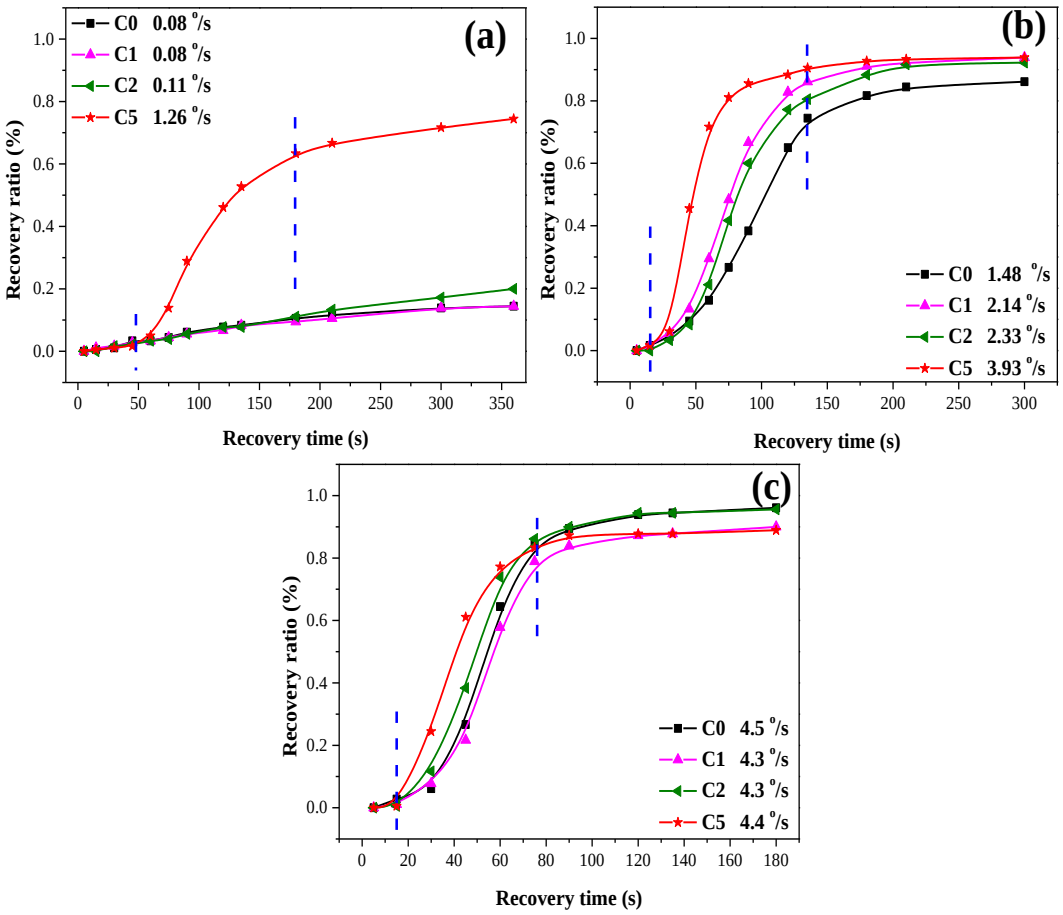

Figure 11

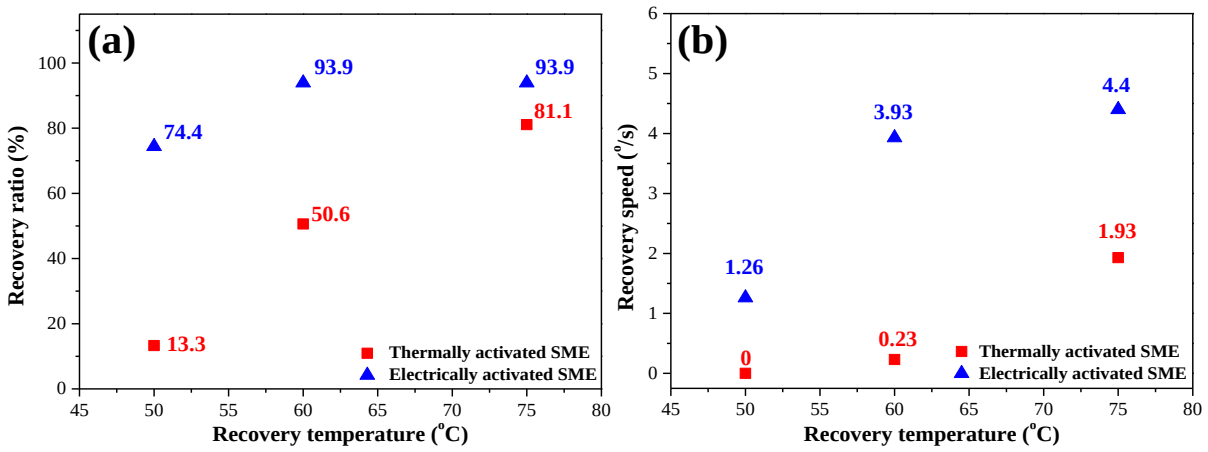

Figure 12

Graphical Abstract

Thermal and electroactive shape memory behaviors of poly(L-lactide)/thermoplastic polyurethane blend induced by carbon nanotubes

Li-na Shao, Jian Dai, Zhi-xing Zhang, Jing-hui Yang, Nan Zhang, Ting Huang, Yong Wang

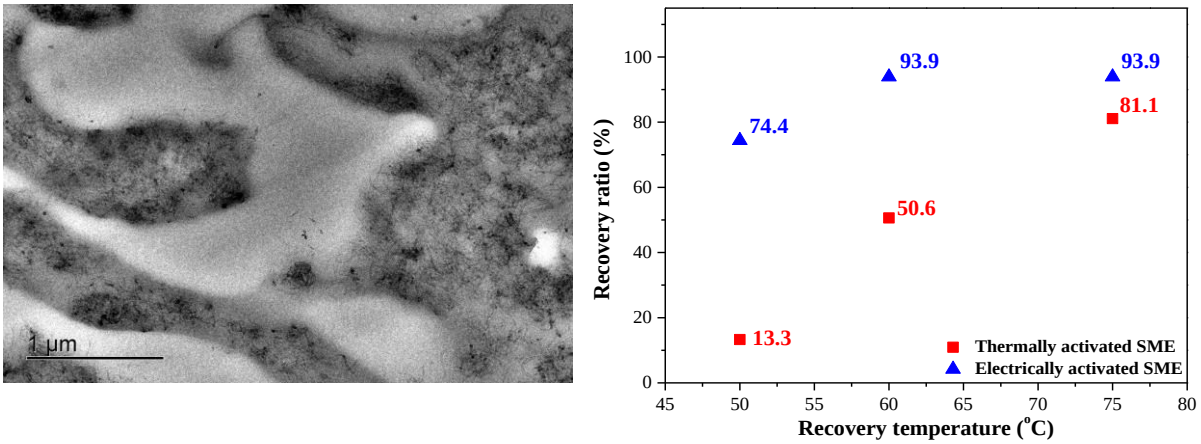

Selectively located CNTs endowed the PLLA/TPU/CNT blend composites with good shape memory behaviors.